


# Improved remote sensing detection of wheat powdery mildew using dual-green vegetation indices

Wei Feng<sup>1,2</sup>  · Wenyng Shen<sup>3</sup> · Li He<sup>1</sup> · Jianzhao Duan<sup>1</sup> ·  
Binbin Guo<sup>1</sup> · Yingxue Li<sup>3</sup> · Chenyang Wang<sup>1,2</sup> ·  
Tiancai Guo<sup>1,2</sup>

Published online: 3 March 2016  
© Springer Science+Business Media New York 2016

**Abstract** In this study, we investigated the possibility of using ground-based remote sensing technology to estimate powdery mildew disease severity in winter wheat. Using artificially inoculated fields, potted plants, and disease nursery tests, we measured the powdery mildew canopy spectra of varieties of wheat at different levels of incidence and growth stages to investigate the disease severity. The results showed that the powdery mildew sensitive bands were between 580 and 710 nm. The best two-band vegetation index that correlated with wheat powdery mildew between 400 and 1000 nm wavelength were the normalized spectrum 570–590 and 536–566 nm bands for the ratio index, and 568–592 and 528–570 nm for the normalized difference index. The coefficients of determination ( $R^2$ ) for both were almost the same. The optimum dual-green vegetation index was constructed based on a calculation of the ratio and normalized difference between the normalized spectrum within the two green bands. The coefficients of determination ( $R^2$ ) of DGSR (584, 550) (dual-green simple ratio) and DGND (584, 550) (dual-green normalized difference) were both 0.845. The inverse models of disease severity performed well in the test process at the canopy scale, and indicated that, compared with the traditional vegetation indices of Lwidth, mND705, ND (SDr, SDb), SIPI, and GNDVI, the novel dual-green indices greatly improved the remote sensing detection of wheat powdery mildew disease. Following these results, combined disease severity and canopy

---

✉ Wei Feng  
fengwei78@126.com

✉ Tiancai Guo  
tcguo888@sina.com

<sup>1</sup> National Engineering Research Centre for Wheat, State Key Laboratory of Wheat and Maize Crop Science, Henan Agricultural University, #62 Nongye Road, Zhengzhou 450002, Henan, People's Republic of China

<sup>2</sup> Collaborative Innovation Center of Henan Grain Crops, Henan Agricultural University, #63 Nongye Road, Zhengzhou 450002, Henan, People's Republic of China

<sup>3</sup> College of Applied Meteorology, Nanjing University of Information Science & Technology, #219 Ningliu Road, Nanjing 210044, Jiangsu, People's Republic of China

spectra were shown to be of enormous value when applied to the accurate monitoring, prevention, and control of crop diseases.

**Keywords** Wheat powdery mildew · Hyperspectral · Dual-green vegetation index · Disease severity · Inversion model

### Abbreviations

SR	Simple ratio
ND	Normalized difference
SD	Simple difference
MSR	Modified simple ratio
SIPI	Structural independent pigment index
SAVI	Soil adjusted vegetation index
TSAVI	Transformed soil adjusted vegetation index
MSAVI	Improved SAVI with self-adjustment factor L
PSRI	Plant senescence reflectance index
CTR2	Carter indices
mND705	Modified ND705 by incorporating reflectance at 445 nm
Depth672	The depth of the absorption feature at 672 nm
Lwidth	Red edge width
SDr	Sum of 1st derivative values within red edge
SDb	Sum of 1st derivative values within blue edge
SDy	Sum of 1st derivative values within yellow edge
ND (SDr, SDb)	Normalized difference between SDr and SDb
ND (SDr, SDy)	Normalized difference between SDr and SDy
PRI	Photochemical reflectance index
RVI	Ratio vegetation index
NDVI	Normalized difference vegetation index
GNDVI	Green normalized difference vegetation index
RVSI	Red-edge vegetation stress index
VARI	Visible atmospherically resistant index
WI	Water index
NSRI	Spectral ratio index in near-infrared shoulder region
PMI	Powdery mildew index
MCARI	Modified chlorophyll absorption ratio index
ARI	Anthocyanin reflectance index
DGND	Dual-green normalized difference
DGSR	Dual-green simple ratio
RGND	Red-green normalized difference
RRSD	Red-red simple difference
ReRSD	Red-edge-red simple difference
PLSR	Partial least squares regression
cDI	Conventional disease index
mDI	Modified disease index
LAI	Leaf area index
R <sup>2</sup>	The coefficients of determination
RMSE	The root mean square error
RE	The relative error

## Introduction

Wheat powdery mildew, caused by the ascomycete fungus *Blumeria graminis* f. sp. *tritici*, is a devastating pathogen of wheat that is found in all major wheat producing countries worldwide. In China, with the promotion of dwarf varieties and the improvement of agricultural conditions, the area and scope of powdery mildew disease incidence is expanding, and the disease severity increasing. For example, in 1990, 50 % of the total area devoted to wheat production was infected with powdery mildew in Henan, China, causing a yield loss of nearly 400 000 tons.

Traditional methods of monitoring wheat powdery mildew have limitations because they mainly rely on artificial field investigations, which are inefficient, subjective, and time-consuming. Therefore, the development of a rapid, non-destructive, real-time monitoring technology could be significant for the precise prevention and control of diseases. Wheat powdery mildew infected by *B. graminis* f. sp. *tritici* results in a layer of white powdery mildew covering the leaf surface, causing mesophyll cell damage, water and chlorophyll content reduction, and leaf yellowing and withering, which then lead to wheat production loss and grain quality degradation (Maxwell et al. 2009; Sharma et al. 2004). Morphological and physiological changes in diseased plants also cause changes in their corresponding spectra, and then provide possibilities for the real-time monitoring of wheat powdery mildew using remote sensing technology (Sankaran et al. 2010).

Several previous studies have shown that the sensitive bands for different crop diseases identified by spectra are mainly located in the visible and near infrared regions (Raikes and Burpee 1998; Wang et al. 2002; Cheng et al. 2010), and that the optimal sensitive bands vary with different crops and different diseases (Zhang et al. 2003; Mahlein et al. 2013). Research on wheat stripe rust showed that the photochemical reflectance index (PRI) is a robust spectral index in quantifying yellow rust infection, and a potential candidate for operational use in the monitoring of this disease (Huang et al. 2007). NSRI (the NIR shoulder region), a simple ratio of reflectance at 890 nm to reflectance at 780 nm, could monitor the deterioration of the wheat blade internal structure caused by the stripe rust pathogen (Liu et al. 2014). In wheat aphid monitoring, it is clear that the sensitive spectral bands are 484–552, 609–619 and 718–770 nm (Luo et al. 2013), and the R800/R450 and R950/R450 can better distinguish the aphid-affected wheat plants (Yang et al. 2009); the normalized difference vegetation index (NDVI), was applied to classify the data into areas showing different levels of disease severity (Franke and Menz 2007). In previous studies monitoring wheat powdery mildew, it was clearly shown that the sensitive spectral bands were 490, 510, 516, 540, 780 and 1300 nm at the leaf level (Graeff et al. 2006), and 580–710 and 750–860 nm at the canopy level (Cao et al. 2013). Red edge parameters, such as the red edge area ( $\Sigma dr_{680-760}$  nm) (Cao et al. 2013) and the red edge width (Lwidth) (Zhang et al. 2012a, b), could better identify wheat powdery mildew disease. Powdery mildew-index (PMI) based on 520, 584 and 724 nm could distinguish powdery mildew from other diseases (Mahlein et al. 2013). The common spectral features as green NDVI (GNDVI), modified chlorophyll absorption ratio index (MCARI) and reflectance of green band also have great potential in estimating the disease severity of wheat powdery mildew (Zhang et al. 2012a, b). For monitoring rice blast, the bands of optimal sensitivity were shown to be near 485 and 675 nm (Kobayashi et al. 2001). Yang et al. (2007) studied  $R_{nir}/R_{red}$ , GNDVI and the soil-adjusted vegetation index (SAVI) for the

detection of brown plant hoppers and leaf-folder infestations in rice plants. In other fruits and vegetables research, NDVI (760, 708) and anthocyanin reflectance index (ARI) can facilitate detection of rhizomania in Sugar Beets (Steddom et al. 2003). Naidu et al. (2009) suggested that different vegetation indices differed in their ability to detect wine disease; MCARI, red-edge vegetation stress index (RVSII) and visible atmospherically resistant index (VARI) performed well. These results suggest that remote sensing using spectral reflectance and indices can be a nondestructive technique to detect infestation caused by disease and pests on different crops. However, the determination of sensitive bands and spectral indices varied between studies.

In recent years, partial least squares regression (PLSR) has been widely used in crop growth monitoring and can overcome the problems of “over-fitting” and collinearity (Herrmann et al. 2011). It is a potential approach with which to determine plant N status of winter wheat (Li et al. 2014) and it can also predict insect infestation on plants (Oumar et al. 2013). In addition, PLSR algorithms can improve monitoring accuracy for wheat powdery mildew at both leaf level and region scale (Zhang et al. 2012a, b, 2014). However, some bands are not informative of the target variable or may even disturb useful signatures, so the PLSR method may not always provide the best solutions (Yoshio et al. 2012). The two-band method, which has the advantage of clear combined bands and various combination forms, is also used to evaluate crop growth status. Exploring innovations of band combination patterns and corresponding coefficients expand their application in crop monitoring. Yoshio et al. (2012) compared various approaches for spectral assessment of canopy nitrogen content in rice and showed that two-band combination of the first derivative is superior to the PLSR method.

Studies on the disease monitoring in other crops have made progress toward the goal of early recognition and prevention to lower the risk of yield loss, reduce pesticide application and cost and protect the environment. However, as these studies mainly relied on limited test conditions and single varieties, it is necessary to confirm and verify quantitative relationships between different varieties and production systems in different years. In addition, the symptoms of wheat powdery mildew occur mostly in the middle and lower parts of the plant, while the canopy spectra is mainly derived from the middle and upper leaves, which results in a weak overall correlation between canopy reflectance and infestation information. Moreover, because related studies were always limited to the single blade level or the qualitative classification of aerial remote sensing (Zhang et al. 2012a, b, 2014; Franke and Menz 2007), it is not known whether any band or vegetation index in different crops and disease could be used to detect powdery mildew stress in wheat using ground-based hyperspectral radiometry.

Artificial inoculation of powdery mildew and measurement of canopy spectra and disease index (DI) in wheat at different levels of infection, will enable us to clearly understand the relationships between spectral bands and disease severity. From this, we can develop a novel vegetation index that will indicate disease development and establish a quantitative estimation model of wheat powdery mildew severity, in order to (1) provide a band reference for multi-channel portable disease monitors, (2) provide quantitative evaluation methods for remote sensing to monitor a large area of wheat powdery mildew damage, and (3) enhance the level of precision for management of agricultural epidemics.

## Materials and methods

### Experimental design

#### *Experiment 1*

The first experiment was conducted at the Science and Education Demonstration Garden, Henan Agricultural University, Zhengzhou, China (34°51'N, 113°35'E) during the 2009–2010 growing season. Four winter wheat cultivars, Yanzhan 4110 and Yumai 34 (susceptible varieties), Aikang 58 and Zhengmai 366 (moderately susceptible varieties), were selected to represent different levels of susceptibility to powdery mildew. The test soil was sandy loam, the 0–0.3 m soil basic indicators were organic matter 8.3 g kg<sup>-1</sup>, total N 0.87 g kg<sup>-1</sup>, available phosphorus 24.44 mg kg<sup>-1</sup>, and available K 124.32 mg kg<sup>-1</sup> prior to planting. Fertilizer application amounts were 240 kg ha<sup>-1</sup> nitrogen, 120 kg ha<sup>-1</sup> P<sub>2</sub>O<sub>5</sub>, and 90 kg ha<sup>-1</sup> K<sub>2</sub>O. Seeds were sown in rows on October 15, 2009. The area of the plot was 20.3 m<sup>2</sup> (7 m long × 2.9 m wide). The planting rate adopted was 135 kg ha<sup>-1</sup>. The experiment was a randomized complete block design with three replications for each treatment. In each plot, cultivation and management were consistent, and the management of other aspects followed standard local practices for wheat production. Based on the amount of inoculum and frequency of inoculation, three treatment levels (heavy, medium, and light) were established, with a non-inoculated area as the control group. Plants were inoculated from the wheat jointing stage to the time when symptoms became obvious. Infection was observed at the heading stage, and canopy spectral testing and sampling was conducted at 5, 15, and 25 days after flowering.

#### *Experiment 2*

The second experiment was conducted in greenhouses located at the National Engineering Research Center for Wheat, Henan Agricultural University, Zhengzhou, China (34°51'N, 113°35'E) during the 2009–2010 growing season. The same four winter wheat cultivars, two susceptible and two moderately susceptible varieties, which were used in Experiment #1 were used here. The test soil was sieved sandy loam. Each square pot (0.25 m × 0.25 m) was filled with 13.5 kg of soil and buried in the soil 20 mm above the ground level. The fertilizer selected was the same as in the first experiment, but twice the amount was used. Seeds were sown by way of dibbling on October 18, 2009. Each pot had ten holes, and two seed were placed in each hole. Powdery mildew inoculations were initiated at the jointing stage. The same three levels of treatment (heavy, medium and light) and the same non-inoculated control from Experiment #1 were used here. Wheat was infected from the heading stage, and the canopy spectral testing and sampling were performed both at the heading stage and 10 days after flowering. The potted wheat plants were moved out of the greenhouse and divided into three groups of one, two, and four pots for spectral measurements. Three methods were determined on two sets of data, for a total of 96 samples.

#### *Experiment 3*

The third experiment was conducted in nursery fields located at the National Engineering Research Center for Wheat, Henan Agricultural University, Zhengzhou, China (34°51'N,

113°35'E) during the 2010–2011 growing season. The three winter wheat cultivars Yanzhan 4110 and Yumai 34 (susceptible varieties) and Aikang 58 (moderately susceptible) were used in this experiment. The test soil was sandy loam, and the 0–0.3 m soil basic indicators were organic matter 16.3 g kg<sup>-1</sup>, total N 1.22 g kg<sup>-1</sup>, available phosphorus 35.65 mg kg<sup>-1</sup>, and available K 114.68 mg kg<sup>-1</sup> before planting. Fertilizer application amounts were 270 kg ha<sup>-1</sup> nitrogen, 120 kg ha<sup>-1</sup> P<sub>2</sub>O<sub>5</sub>, and 90 kg ha<sup>-1</sup> K<sub>2</sub>O. Disease conditions were the same as in Experiment #1, with a total of four treatments and two replications. Seeds were sown in rows on October 15, 2010, and the area of the plot was 8.1 m<sup>2</sup>. The planting rate was the same as that used in Experiment #1. Cultivation and management practices were consistent for each plot, and other aspects of management followed standard local practices for wheat production. Infection began from the booting stage, and canopy spectral testing and sampling were conducted at heading and 10 days after flowering.

## Inoculations

### *Leaf inoculation*

Based on the experimental design, infected plants showing symptoms of powdery mildew in the greenhouse nursery were dug up and shaken over the top of plants in the plot to be inoculated. The diseased plants were then placed horizontally in the middle and lower part of the wheat plants. Leaf inoculation was undertaken every 2 days.

### *Inoculation of potted plants*

When the potted plants had reached full size in the greenhouse nursery area, they were inoculated using diseased potted plants as described in the previous section, and then the potted plants were set in the plot. To ensure uniform inoculation in the plot, their positions were changed every 2 days.

## Canopy spectral measurements

All canopy spectral measurements were taken from a height of 1.0 m above the canopy, and the diameter of the ground visual field range was 0.44 m on a sunny and windless day (or when the wind speed was low), between 10:00 and 14:00 (Beijing local time), using a FieldSpec HandHeld spectrometer (Analytical Spectral Devices Inc., USA). The spectrometer was operated with a field angle of 25°, a spectral sampling interval of 1.4 nm, and spectral resolution of 3.0 nm in the band region between 325 and 1075 nm. A 0.4 m × 0.4 m BaSO<sub>4</sub> calibration panel was used for calculating the black and baseline reflectance. In each experiment, data were obtained on several different days corresponding to the main growth stages. Ten spectra were recorded as a sample at each sampling point, the mean value of which was calculated as the spectral reflectance of the point.

## Assessment of disease index

Disease incidence rating surveys were collected simultaneously after spectral data acquisition. Twenty plants were randomly selected to assess the severity of powdery mildew in

the range of about 0.6 m<sup>2</sup> of the spectral test location. In the pot experiments we used all leaves of the whole plant and the severity to indicate the incidence condition. The severity was the percentage of the incidence area of wheat leaf relative to the total leaf area using a square grid. Powdery mildew severity was assessed on a 0–9 scale as follows: 0, 1, 10, 20, 30, 45, 60, 80, 100 %. The average DI was calculated with the following equation (Cai et al. 2007):

**Table 1** The common spectral parameters used in this study

Spectral parameters	Formulae	References
SIPI	$(R_{800} - R_{445}) / (R_{800} - R_{680})$	Peñuelas et al. (1995)
TSAVI	$\frac{a \times (R_{NIR} - a \times R_{RED} - b)}{a \times R_{NIR} + R_{RED} - ab}$	Baret et al. (1989)
MSAVI	$\frac{1}{2} \times (2 \times R_{800} + 1 - \sqrt{(2 \times R_{800} + 1)^2 - 8 \times (R_{800} - R_{670})})$	Qi et al. (1994)
PSRI	$(R_{680} - R_{500}) / R_{750}$	Merzlyak et al. (1999)
CTR2	$R_{695} / R_{760}$	Carter and Miller (1994)
mND705	$(R_{750} - R_{705}) / (R_{750} + R_{705} - 2 \times R_{445})$	Sims and Gamon (2002)
MCARIB	$\frac{1.5 \times (1.2 \times (R_{800} - R_{550}) - 2.5 \times (R_{670} - R_{550}))}{\sqrt{(2 \times R_{800} + 1) - (6 \times R_{800} - 5 \times \sqrt{R_{670}}) - 0.5}}$	Haboudane et al. (2004)
Depth672	$1 - \frac{R_{672}}{(R_{672} - R_{670}) + (R_{670} - R_{672}) \times \frac{R_{672}}{R_{670}}}$	Kokaly and Clark (1999)
Lwidth	$R(\lambda) = R_s - (R_s - R_0) \exp\left(\frac{-(\lambda_0 - \lambda)^2}{2\sigma^2}\right)$	Miller et al. (1990)
SDr	$\Sigma dr680-760$	Gong et al. (2002)
SDb	$\Sigma dr490-550$	Gong et al. (2002)
SDy	$\Sigma dr550-650$	Gong et al. (2002)
ND (SDr, SDb)	$(SD_r - SD_b) / (SD_r + SD_b)$	Gong et al. (2002)
ND (SDr, SDy)	$(SD_r - SD_y) / (SD_r + SD_y)$	Gong et al. (2002)
MSR	$(R_{800} / R_{670} - 1) / (R_{800} / R_{670} + 1)^{0.5}$	Haboudane et al. (2004)
PRI	$(R_{531} - R_{570}) / (R_{531} + R_{570})$	Gamon et al. (1992)
GNDVI	$(R_{800} - R_{550}) / (R_{800} + R_{550})$	Gitelson et al. (1996)
SAVI	$1.5 \times (R_{800} - R_{670}) / (R_{800} + R_{670} + 0.5)$	Huete (1988)
RVI (800, 670)	$R_{800} / R_{670}$	Baret and Guyot (1991)
RVSI	$(R_{714} + R_{752}) / (2 - R_{733})$	Merton and Huntington (1999)
VARI	$(R_{550} - R_{670}) / (R_{550} + R_{670} - R_{480})$	Gitelson et al. (2002)
WI	$R_{900} / R_{970}$	Peñuelas et al. (1997)
NSRI	$R_{890} / R_{780}$	Liu et al. (2014)
PMI	$(R_{520} - R_{584}) / (R_{520} + R_{584}) + R_{724}$	Mahlein et al. (2013)
RVI (800, 450)	$R_{800} / R_{450}$	Yang et al. (2009)
RVI (950, 450)	$R_{950} / R_{450}$	Yang et al. (2009)
MCAR1a	$[(R_{700} - R_{670}) - 0.2 \times (R_{700} - R_{550})] \times (R_{700} / R_{670})$	Daughtry et al. (2000)
ARI	$(R_{550})^{-1} - (R_{700})^{-1}$	Gitelson et al. (2001)

$$DI = \frac{\sum xf}{n \sum f} \times 100$$

where  $x$  is the value of every incidence level,  $n$  is the highest incidence level (in this work,  $n = 9$ ), and  $f$  is the total number of leaves of each degree of disease severity. The definition and calculation of the formula for the conventional DI (conventional DI, cDI) was based on previously established studies. Powdery mildew on wheat spreads from the lower leaves upward as disease progresses. Therefore, prior to the appearance of moderate disease incidence, symptoms are mostly centered on the lower parts of the plant, whereas the canopy spectrum is mainly affected by the middle and upper leaves. Consequently there is a significant deviation by means of canopy spectral detection, which will have a strong impact on the early identification and prevention of disease. In this study, the conventional DI divided by the leaf area index (LAI) of the corresponding plot indicated the degree of DI per unit leaf area, which was defined as the modified DI (modified DI, mDI). It is straightforward to compare the influence of disease severities on the canopy spectra under different LAI, in order to decrease the influence exerted by population structure diversity on the disease severity estimation. Correlation analysis of the wheat DI with canopy spectral data confirmed that mDI was the appropriate expression indicator for the canopy spectra.

## Data analysis

We used the Savitaky–Golay smoothing method in the MATLAB program to smooth the raw spectral data (Turton 1992). The common spectral parameters that were selected to establish monitoring models based on their correlation with mDI are listed in Table 1. Previous studies reported that the image normalization and reflectance ratio were able to suppress both additive and multiplicative noises. A transformation calculation was applied to measure the change magnitude of spectral features between different conditions (Zhang et al. 2012a, b, 2014). To suppress the possible difference of the illumination, stages, canopy and blade structure, we then normalized all spectra curves of the diseased plants by dividing them by the reflectance of healthy plants. The reflectance ratio was calculated as:

$$R_{Ni} = R_{Di}/R_{Hi}$$

where  $R_{Ni}$  is the normalized spectrum for band  $i$ ,  $R_{Di}$  is the original reflectance of diseased plots at the band, and  $R_{Hi}$  is the original reflectance of healthy plots at the band.

The two-band combinations were calculated using all possible combinations of two wavebands ( $\lambda_1$  and  $\lambda_2$ ) in the 400–1000 nm region. These consisted of three types of indices: (1) a simple ratio index (SR), (2) a normalized difference index (ND), and (3) a simple difference index (SD). In addition, we further studied the following three relationships: (1) the two-band original reflectance ratio, and normalized difference and simple difference index with mDI, (2) the normalized spectrum simple ratio, and normalized difference and simple difference index with cDI, and (3) the normalized spectrum simple ratio, and normalized difference and simple difference index with mDI. Programming was performed in the MATLAB language environment. We selected data from Experiments 1 and 2 involving different species, test systems, and grades of the incidence for modeling analysis, and used the independent experimental data from Experiment 3 to test the above monitoring models. We used the correlation coefficient ( $R^2$ ), the root mean square error (RMSE), and the relative error (RE) between predicted and observed values to evaluate model accuracy.



## Results

### Variation in features of wheat canopy spectra with differing severities of powdery mildew disease

Yanzhan 4110 (susceptible) and Aikang 58 (moderately susceptible) in Experiment 1 were selected to show the impact of disease severity on canopy spectra (Fig. 1). Yanzhan 4110 had the following characteristics: moderate tillering ability, small groups, a relatively full reflection of the disease information in the lower part of the plant on canopy spectra, obvious disease symptoms characteristic of a susceptible variety, and large spectral differences between different grades of infection. However, Aikang 58 had the opposite characteristics: strong tillering ability, larger groups, less obvious reflection of disease symptom information on spectra than Yanzhan 4110, relatively weak disease symptoms characteristic of a moderately susceptible variety, lower level of disease incidence, and smaller spectrum differences between different grades of infection. With an increase in the mDI, spectral reflectance in the visible bands 350–710 nm gradually increased, and the 620–680 nm bands were the most conspicuous (Yanzhan 4110,  $P < 0.001$ ; Aikang 58,  $P < 0.05$ ). Reflectance in the red edge region did not change significantly, but the slope steepened, and the valley weakened. The reflectance did not show a certain noticeable change rule in the near-infrared region, but it had a larger amplitude as for the disease treatments, especially in the susceptible variety Yanzhan 4110, with a mean value of 31.2–40.6 % in the range of 780–1075 nm.

### Correlation between wheat powdery mildew severity and canopy spectra

The overall performance of the correlation coefficient between canopy spectra and the cDI was low. A good correlation was mainly in the 550–700 nm region ( $r < 0.46$ ), and the effect for the pot experiments ( $n = 96$ ) was markedly superior to that for the field trials ( $n = 51$ ) (Fig. 2). This could be because the pot experiments were conducted in a controlled climate with fast onset, a high disease incidence, and short lag periods between disease symptoms on the upper and lower parts of the plants, and therefore the plant disease information was reflected more fully in the canopy spectra. Compared with the

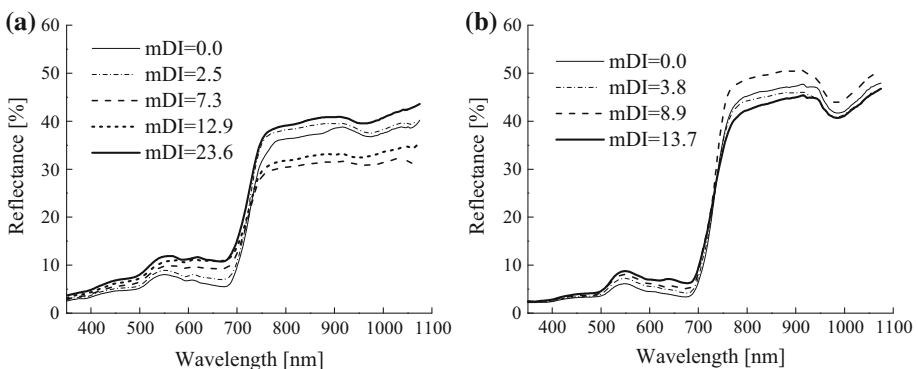
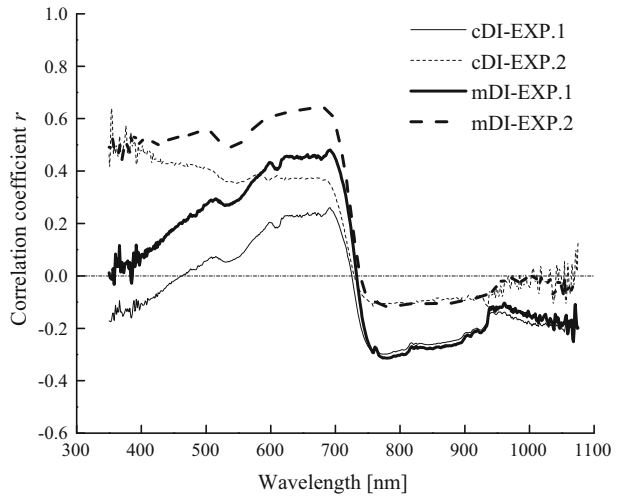


**Fig. 1** Changes in the original spectrum reflectance under different modified disease indices (mDI) in winter wheat with Yanzhan 4110 (a) and Aikang 58 (b)

**Fig. 2** Correlation of the disease indices of wheat infected with powdery mildew to canopy original spectral reflectance. *cDI* conventional disease index, *mDI* modified disease index, *EXP. 1* experiment one (field experiment), *EXP. 2* experiment two (pot experiment)



cDI, the correlation between the mDI and the original spectral reflectance was significantly improved, which also showed the advantage of pot experiments over field experiments. There were positive correlation coefficients in the 350–750 nm range, especially for 580–710 nm ( $r \in (0.5 - 0.7)$ ,  $P < 0.001$ ) with a higher value that could be considered to be disease-sensitive bands. The near-infrared region, 750–1075 nm, showed an overall negative but poor correlation ( $r < 0.30$ ). This indicated that mDI mitigated the influence on the correlation analysis between spectrum and cDI due to the leaf area differences, significantly improving the abilities of the canopy spectrum in response to and recognition of the disease status.

### Correlation between wheat powdery mildew severity and common spectral parameters

Based on the reported characteristic spectral bands and vegetation indices, we used the integrated wheat DI and canopy spectral parameters in the different test systems, wheat varieties, and growth stages to conduct regression analyses. The relevant analysis of data for the different varieties from the open-field experiment ( $n = 51$ ) and the nursery greenhouse ( $n = 96$ ) is shown in Table 2. This analysis showed that expect for SDb, PMI, RVSI, ARI and WI, the remaining twenty-three spectral indices were significantly correlated with mDI ( $P < 0.001$ ), and that the correlations of mDI were significant better than those of cDI. Because the nursery test system showed a big difference compared with the open-field experiment in the ecological environment and disease characteristics, a comprehensive analysis of Experiments 1 and 2 was needed. The slope and intercept of the fitting equations were different from each other to some extent under the different production test systems, resulting in a much weaker correlation between the majority of spectral parameters and the DI. However, Lwidth (the red edge width) still showed a flat correlation coefficient with a single test system, up to 0.854 ( $P < 0.001$ ). The following spectral parameters: mND705, ND (SDr, SDb), SIPI, GNDVI, and CTR2 also gave good correlation coefficients ( $P < 0.001$ ), and the respective values of  $r$  were  $-0.545$ ,  $-0.585$ ,  $0.538$ ,  $0.535$ , and  $0.520$ . Figure 3 shows that the slope and intercept of the Lwidth of the

**Table 2** Correlation coefficients between canopy spectral indices and modified disease indices in winter wheat

Spectral parameters	cDI			mDI		
	EXP. 1	EXP. 2	EXP. 1 & 2	EXP. 1	EXP. 2	EXP. 1 & 2
SIPI	0.549***	0.467***	0.375***	0.844***	0.815***	0.538***
TSAVI	0.466***	0.411***	0.173*	0.789***	0.756***	0.509***
MSAVI	-0.442**	-0.407***	0.168*	-0.777***	-0.748***	-0.484***
PSRI	0.574***	0.297**	0.253**	0.847***	0.789***	0.465***
CTR2	0.476***	0.392***	0.164*	0.797***	0.754***	0.520***
mND705	-0.488***	-0.287**	-0.192*	-0.787***	-0.749***	-0.545***
MCARib	-0.574***	-0.375***	-0.238**	-0.865***	-0.786***	-0.461***
Depth672	-0.463***	-0.481***	-0.266**	-0.795***	-0.752***	-0.473***
Lwidth	0.694***	0.492***	0.457***	0.881***	0.832***	0.854***
SDr	-0.328*	-0.275**	0.153	-0.360**	-0.406***	-0.386***
SDb	0.078	0.126	-0.015	0.305*	0.234*	0.267**
SDy	0.374**	0.360***	-0.245**	0.294*	0.707***	0.509***
ND (SD <sub>r</sub> , SD <sub>b</sub> )	-0.394**	-0.363***	0.046	-0.733***	-0.667***	-0.585***
ND (SD <sub>r</sub> , SD <sub>y</sub> )	0.398**	0.397***	0.176*	0.269	0.835***	0.527***
MSR	-0.318*	-0.417***	0.298***	-0.540***	-0.633***	-0.393***
PRI	0.469***	0.355***	-0.312***	0.614***	0.656***	0.450***
GNDVI	-0.309*	-0.454***	0.140	-0.545***	-0.612***	-0.535***
SAVI	-0.381**	-0.411***	0.233**	-0.594***	-0.664***	-0.506***
RVI (800, 670)	-0.280**	-0.412***	0.311***	-0.504***	-0.613***	-0.344***
RVSI	-0.181	-0.002	-0.064	-0.106	-0.004	-0.058
VARI	-0.559***	-0.296**	0.362***	-0.671***	-0.630***	-0.368***
WI	-0.217	0.087	0.019	-0.192	0.181	0.085
NSRI	0.668***	0.505***	0.255**	0.711***	0.565***	0.495***
PMI	0.013	0.053	-0.171*	0.175	0.235*	0.262**
RVI (800, 450)	-0.164	-0.471***	0.260**	-0.423**	-0.580***	-0.403***
RVI (950, 450)	-0.257	-0.423***	0.335***	-0.473***	-0.621***	-0.357***
MCAR <sub>1a</sub>	-0.320**	-0.267**	0.207*	-0.350*	-0.446***	-0.391***
ARI	0.589***	-0.277**	-0.295***	0.529***	-0.188	0.051

*cDI* conventional disease index, *mDI* modified disease index, *EXP. 1* experiment 1, *EXP. 2* experiment 2, *EXP. 1 & 2* comprehensive experiments 1 and 2

\*  $P < 0.05$ ; \*\*  $P < 0.01$ ; \*\*\*  $P < 0.001$

Gaussian model in the regression equations for Experiment 1 ( $n = 51$ ) and Experiment 2 ( $n = 96$ ) were not significantly different ( $P > 0.05$ ). Therefore, the unified regression equation can be used to express DI changes per unit leaf area, and the coefficient of determination ( $R^2$ ) and the RMSE were 0.709 and 3.64, respectively. Despite the relatively better compatibility of spectral parameters mND705, ND (SD<sub>r</sub>, SD<sub>b</sub>), SIPI, GNDVI, and CTR2 in Experiments 1 and 2 integrated relevant analysis ( $|r| > 0.5$ ), the differences in the slope and intercept of the regression equation combined in the two trials were too large ( $P < 0.01$ ) to fit by virtue of the uniform regression equation. We chose intuitively

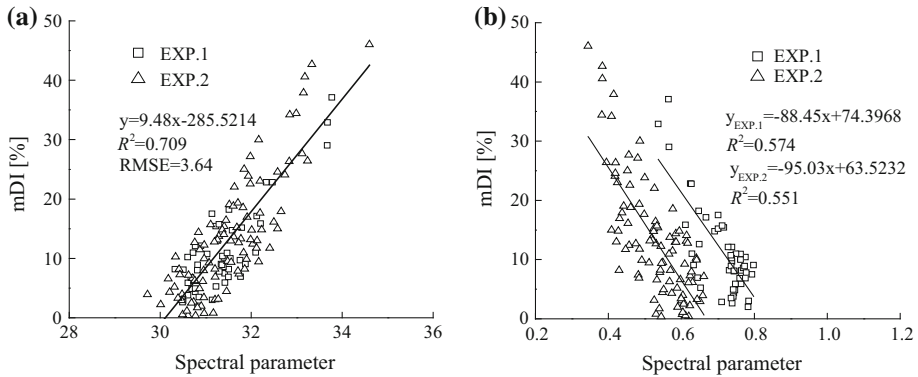


**Fig. 3** Quantitative relationships of the modified disease indices (mDI) and conventional spectral parameters of Lwidth (a) and mND705 (b) in winter wheat

mND705 as representative to show the differences between the two test systems in the scatter plot diagram (Fig. 3b).

### Correlation between wheat powdery mildew severity and two-band combination indices

The results showed poor correlation for all the bands in the near infrared regions between two bands in the original spectrum simple ratio, normalized difference and simple difference index and mDI. However, the coefficients of determination were low ( $R^2 < 0.50$ ). The bands that showed a good correlation between the normalized spectrum simple ratio, normalized difference and simple difference index, and cDI were also distributed in the near infrared region, and showed lower coefficients of determination ( $R^2 < 0.60$ ). The bands that showed a better correlation between the normalized spectrum simple ratio, normalized difference and simple difference index and mDI in the visible region and red edge region, had the highest coefficient of determination,  $R^2 > 0.75$ . Among these, the ratio index band combinations that were well correlated with mDI were 570–590 and 536–566 nm, 604–616 and 540–560 nm, and 626–680 and 540–558 nm—three regions of band combinations ( $R^2 > 0.70$ ) (Fig. 4c). The normalized difference index band combinations that were well correlated with mDI were 568–592 and 528–570 nm, and 604–684 and 538–560 nm—two regions of band combinations ( $R^2 > 0.70$ ) (Fig. 4f). The simple difference index band combinations that were well correlated with mDI were 590–616 and 624–640 nm, and 590–612 and 656–734 nm—two regions of band combinations ( $R^2 > 0.70$ ) (Fig. 4i).

Among these band combinations, the ratio vegetation index with the highest correlation with mDI for wheat powdery mildew consisted of 584 and 550 nm in the green region; that is, DGSR (584, 550) (dual-green simple ratio) was better than RGSR (670, 550) (red-green simple ratio) in the red and green regions. The normalized difference index included the same two-band combinations, similarly, DGND (584, 550) (dual-green normalized difference) was better than RGND (670, 550) (red-green normalized difference) in the red and green regions. However, the simple difference index band combination was comprised of 634 and 604 nm in the red region, namely RRSD (634, 604) (red–red simple difference), which indicated that the single test performed better than the combined test. ReRSD (720,

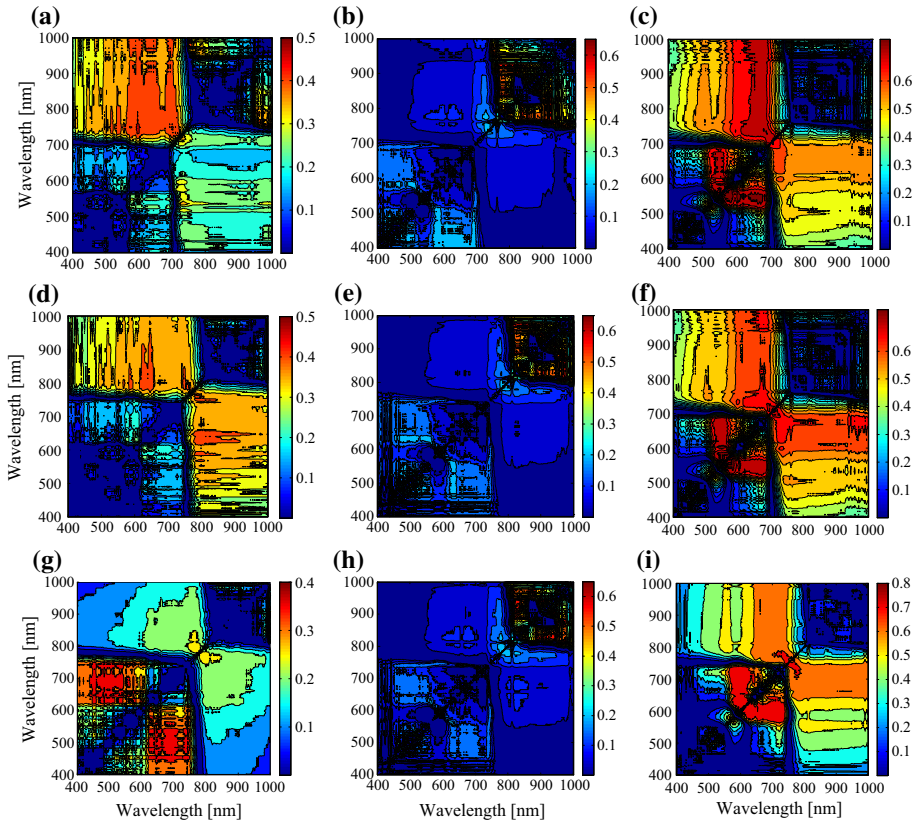


**Fig. 4** Correlations of three types of vegetation indices (SR, ND, and SD) with the two kinds of disease indices (cDI and mDI) in winter wheat. **a** Correlations between SR and mDI based on canopy original spectral reflectance. **b** Correlations between SR and cDI based on canopy relative spectral reflectance. **c** Correlations between SR and mDI based on canopy relative spectral reflectance. **d** Correlations between ND and mDI based on canopy original spectral reflectance. **e** Correlations between ND and cDI based on canopy relative spectral reflectance. **f** Correlations between ND and mDI based on canopy relative spectral reflectance. **g** Correlations between SD and mDI based on canopy original spectral reflectance. **h** Correlations between SD and cDI based on canopy relative spectral reflectance. **i** Correlations between SD and mDI based on canopy relative spectral reflectance

604) (red-edge-red simple difference) showed that the combined test performance was close to that of the single test. The normalized spectrum simple ratio and normalized difference indices consisted of 584 and 550 nm and gave the same  $R^2$  with powdery mildew severity. We only selected DGND (584, 550) to exhibit quantitative change patterns of canopy reflectance spectra with disease severity. Figure 5 shows that DGND (584, 550) generated  $R^2 = 0.845$  of the mDI model for wheat powdery mildew, which was superior to the wheat powdery mildew models of RGND (670, 550), RRSD (634, 604) and ReRSD (720, 604).

Given the simplicity and practicality of the three types of indices based on normalized spectrum data, SR, ND and SD can be simply calculated from reflectance spectral data across health and disease plots, and formulated as follows:

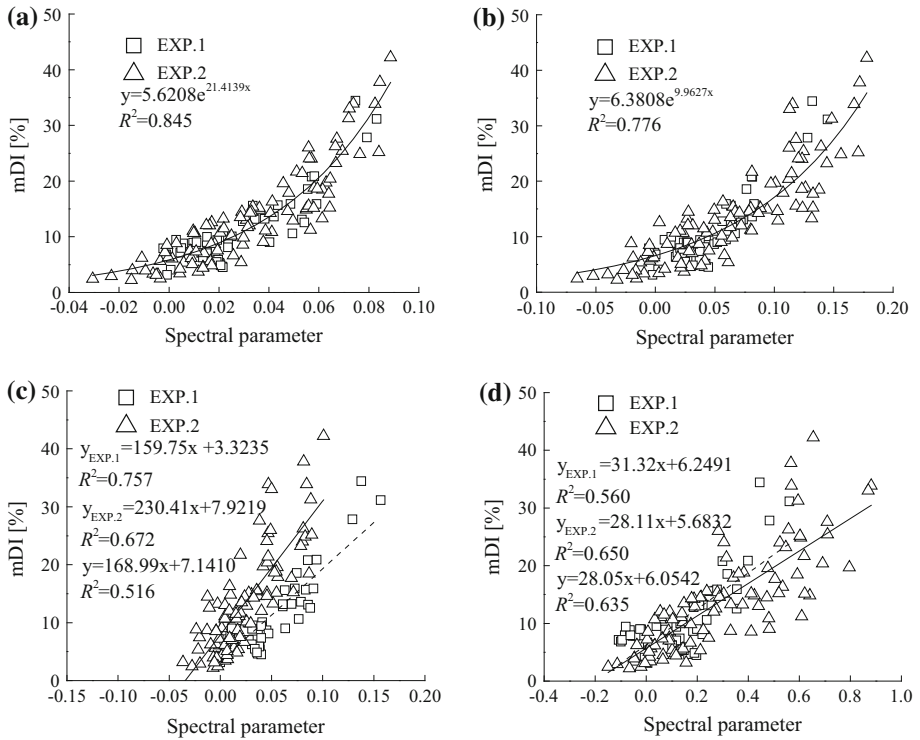


**Fig. 5** Quantitative relationships of the modified disease indices (mDI) and vegetation index based on relative spectrum in winter wheat. **a** DGND (584, 550), **b** RGND (670, 550), **c** RRSd (634, 604), **d** ReRSd (720, 604)

$$\text{DGSr (584, 550)} = (R_H550/R_H584) \times (R_D584/R_D550)$$

$$\text{RGSr (670, 550)} = (R_H550/R_H670) \times (R_D670/R_D550)$$

$$\text{DGND (584, 550)} = (R_D584 \times R_H550 - R_D550 \times R_H584) / (R_D584 \times R_H550 + R_D550 \times R_H584)$$

$$\text{RGND (670, 550)} = (R_D670 \times R_H550 - R_D550 \times R_H670) / (R_D670 \times R_H550 + R_D550 \times R_H670)$$

$$\text{RRSd (634, 604)} = (R_D634/R_H634) - (R_D604/R_H604)$$

$$\text{ReRSd (720, 604)} = (R_D720/R_H720) - (R_D604/R_H604)$$

where  $R_H$  and  $R_D$  are the reflectance value of healthy and diseased wheat, respectively.

### Model testing and inspection

In order to examine the reliability and generalization of the above quantitative identification model, we used data from Experiment 3 ( $n = 40$ ) to verify the preferred equations, and testing was done through three indicators of precision ( $R^2$ ), RMSE, and the mean relative error (RE). We also made a predicted and observed values 1:1 diagram to intuitively show the predictive power of the model. Due to similar test results of simple ratio with normalized difference of 584 and 550 nm or 670 and 550 nm for the canopy normalized spectrum, we chose the normalized difference type as representative of the results.

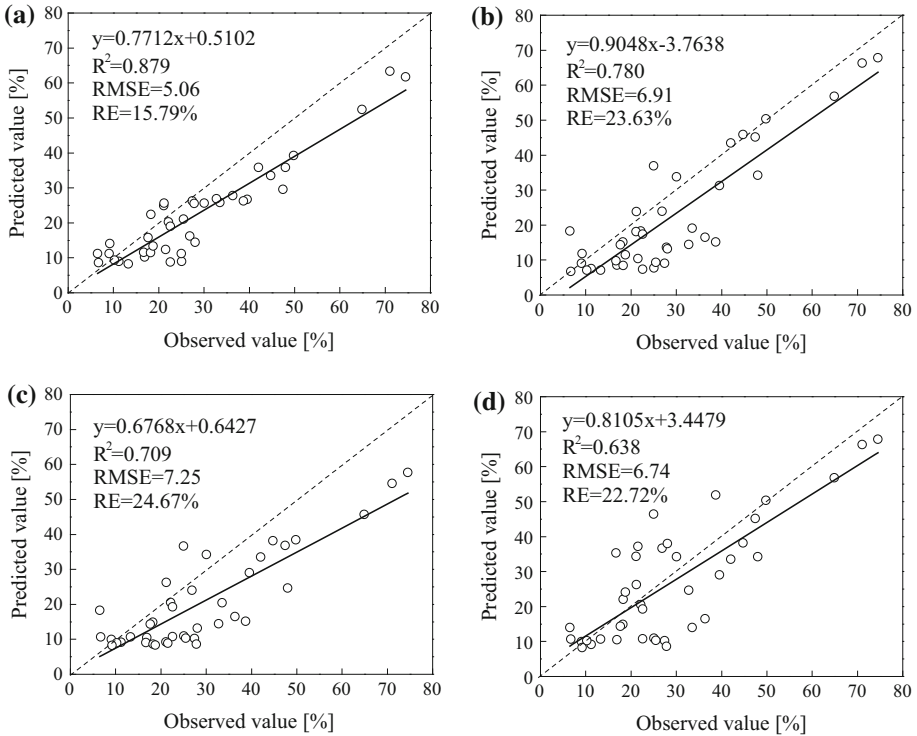


**Fig. 6** Comparisons of predicted and observed disease indices of powdery mildew disease in wheat ( $n = 40$ ). **a** DGND (584, 550), **b** RGND (670, 550), **c** RRSD (634, 604), **d** Lwidth

Figure 6a shows that for the canopy normalized spectrum, the DGND (584, 550) models gave better test results with  $R^2 = 0.88$  and RE 15.79 %, and the predicted values were lower than the measured values in general. Meanwhile, RGND (670, 550), RRSD (634, 604) and Lwidth models generated relatively poor results with REs of 23.63, 24.67 and 22.72 %, respectively. Because the incidence and existing disease characteristics for powdery mildew differed in different test systems, and the original spectrum was influenced by the test environment and other factors, the number of suitable spectral indices monitoring the disease was relatively small. It can mitigate the heterogeneous impact of species, growth stages, and different test conditions on monitoring model by calculating the relative spectral indices.

## Discussion

### Spectral characteristics and sensitive bands under different disease conditions

Infected plants showed a reduction in biomass, chlorophyll levels, and water content, but an increase in the corresponding optical reflectance, and this is the same for different crops and diseases (Cheng et al. 2010). Because of various dimensions of the spectrum test, the canopy reflectance level fell (Guo et al. 2009; West et al. 2003) and leaf reflectance

increased (Jing et al. 2009) in the near infrared region. The visible and near infrared bands showed distinct reaction characteristics to the presence of disease, but the sensitivities of the two region bands to the disease were different, which means that differences in the visible bands were more obvious than in the near-infrared band with a smaller change of spectral reflectance (Jing et al. 2009; Zhang et al. 2012a, b). This is similar to results from previous studies of powdery mildew on single leaf blades in wheat, where it was pointed out that the sensitive band was 520–720 nm, and disagreement appears in the 780–900 nm bands (Peñuelas et al. 1995; Zhang et al. 2012a, b). There have also been inconsistent results showing a closer correlation between the near-infrared reflectance and the disease severity (Guo et al. 2009). In this paper, we have shown that the disease sensitive bands are between 580 and 710 nm, and are significantly positively correlated with powdery mildew disease severity. While in the near infrared region, reflectance was negatively correlated with disease severity on the whole, and the correlation was poorer. Thus, it was not possible to use near infrared as the sensitive bands for disease recognition.

### Disease detection of red-edge spectral characteristic parameters

The red edge is indicative of vegetation nutrition, growth, moisture, and leaf area. When vegetation is aging or suffering from pests or disease, the red edge position appeared to make a “blue shift”; the red edge amplitude decreased and the red edge area was reduced (West et al. 2003). The correlation between the red and blue edge area ratio and disease severity was significantly negative (Guo et al. 2009; Jing et al. 2009), leading to better regression modeling of red edge parameters and DI. The study of wheat powdery mildew found that the red edge width was highly correlated with disease severity (Zhang et al. 2012a, b), but such a discovery was limited to the single leaf level. Our tests demonstrated that after the powdery mildew fungus infects wheat, the canopy spectral red valley features weakened and Lwidth increased. Lwidth in the biennium unified modeling showed a flat correlation with the single test system ( $r = 0.854$ ,  $P < 0.001$ ), whereas the other common original spectrum parameters had poorer comparability in the annual modeling.

In our field experiments, reflectance at 350–550 nm showed rather large differences between the two seasons, and there was a significantly positive correlation in 550–710 nm and a non-obvious negative correlation in the near-infrared band. The greenhouse pot experiment, however, had a negative correlation ( $|r| < 0.3$ ), which was quite different from previous results with wheat stripe rust ( $|r| \in 0.6 - 0.8$ ) (Guo et al. 2009). This could be due to differences in disease types and test systems, and more variable factors that influence diseases in the near-infrared spectrum than in the visible spectrum, so the disease-specific spectral performance was not stable enough. This may explain why many disease-related indices in previously reported disease detection case studies (e.g., Depth672, SDr, RVSI, PMI, MCARIa and ARI) show only weakly correlation ( $-0.5 < r < 0.5$ ) with wheat powdery mildew.

### Disease detection of the dual-green vegetation index

As a result of the bottom-up characteristic of the infection and spread of powdery mildew, it is very difficult to detect disease symptoms using the canopy spectrum. Previous studies have shown that the correlation between canopy reflectance and powdery mildew DI is generally poor, and is not as obvious as that between canopy reflectance and growth parameters such as nitrogen and chlorophyll. Consequently, some researchers turned to the use of partial least square regression and neural networks, to monitor disease (Zhang et al.



2014; Sankaran et al. 2010), which made it difficult to provide band references for the multi-channel portable disease monitor and was barely conducive to production-oriented applications.

Previous disease detection case studies used the combinations of green and red (GNDVI and VARI) or red edge bands (PMI and AVI) to detect crop diseases (Sankaran et al. 2010; Zhang et al. 2012a, b; Mahlein et al. 2013). The ratio of 550–600 and 500–550 nm was screened against inverse crop parameters (Tian et al. 2011). The photochemical reflectance index PRI (531,570), comprised of green bands, was also investigated to monitor winter wheat stripe rust at the canopy level (Huang et al. 2007). However, these green-related indices performed poorly ( $-0.55 < r < 0.55$ ) for monitoring powdery mildew at canopy scale in the studies, which may be related to the type of disease and the scale of monitoring among different test system. The spectral bands that showed a close correlation with powdery mildew disease were mainly located in the green band caused by the white powdery mycelium covering the leaf surface, which was similar to increasing the light intensity (Mahlein et al. 2013). This could be because after infection, there is a decrease both in chlorophyll content and light carrier received, which is closely linked to the green band in the visible region. This requires us to explore the combination of the green band to improve the specificity and effectiveness in monitoring powdery mildew. We used the normalized spectrum index to weaken the impact on disease stages and test conditions. The results showed that the ratio of the normalized spectrum from 570–590 to 536–566 nm and the normalized difference between 568–592 and 528–570 nm was strongly associated with the DI ( $R^2 > 0.75$ ). The dual-green vegetation index DGND (584, 550) established in this paper improved the correlation with disease severity ( $R^2 = 0.845$ ,  $P < 0.001$ ), which showed a better compatibility. DGSR (584, 550) also gave similar results. The above two novel dual-green vegetation indexes significantly improve estimation precision ( $R^2 = 0.709$ – $0.845$ ) compared with optimal common vegetation index Lwidth. However, the vegetation indices RRSD (634, 604) and ReRSD (720, 604) from our work in the red band performed poorly in the correlation with disease severity ( $R^2 < 0.65$ ), and also showed poorer compatibility in the two trials. The dual-green vegetation index provides a new way of thinking and analysis for spectral monitoring of plant diseases, and also allows us to perform a band selection for the multi-channel portable spectrum monitor.

Although the two-band method is widely used in crop growth monitoring, it has some shortcomings (Atzberger et al. 2015). Based on different crops and growth conditions, the appropriate band combination patterns should be constantly explored to monitor specific targets. The innovation of this study is the improved two-band method using the conversion of spectral data and detection index. This improved method turned the original spectrum into a normalized spectrum and the DI into a DI/LAI. Through applying this approach, we obtain optimized green band combinations and the best estimation model for powdery mildew disease severity, which can provide a specific band reference for multi-channel portable disease monitors. However, it remains to be seen whether such a system can stand up to extensive testing in the form of more diverse ecological sites, production levels, and multiple varieties. This will be extremely important for the early detection, prevention, and treatment of crop diseases.

## Conclusions

In this study, we used wheat canopy spectral data collected in an open field and in the greenhouse. The two experiments involved different types of onset environment, disease characteristics, and symptom performances, and were complementary to each other. We have clearly shown that the spectral bands sensitive to wheat powdery mildew are 580–710 nm, and the accuracy of the green bands combination is higher ( $R^2 > 0.80$ ). The dual-green vegetation index, the dual-green normalization difference [DGND (584, 550)], can more effectively monitor the occurrence status of powdery mildew in the middle and late growth stages of wheat, and these models with higher precision can serve as the best estimation model for powdery mildew disease severity. These results will provide empirical evidence for the monitoring of diseases and pests through the use of remote sensing technology.

**Acknowledgments** This research was supported by grants from the National Natural Science Foundation of China (30900867), the Special Fund for Agro-scientific Research in the Public Interest (201203096, 201303109), the Twelfth Five-Year National Science & Technology Pillar Program (2015BAD26B01, 2013BAD07B07), and the Key Scientific Research Project of Colleges and Universities in Henan Province, China (15A210010).

**Author contributions** Wei Feng, Wenying Shen, Tiancai Guo conceived and designed the research. Wei Feng, Wenying Shen, Yingxue Li and Chenyang Wang analyzed the data and wrote the manuscript. Jianzhao Duan, Li He and Binbin Guo provided data and data acquisition capacity.

## Compliance with ethical standards

**Conflict of Interest** The authors declare that they have no conflict of interest.

## References

- Atzberger, C., Darvishzadeh, R., Immitzer, M., Schlerf, M., Skidmore, A., & Maire, G. (2015). Comparative analysis of different retrieval methods for mapping grassland leaf area index using airborne imaging spectroscopy. *International Journal of Applied Earth Observation and Geoinformation*, *43*, 19–31.
- Baret, F., & Guyot, G. (1991). Potentials and limits of vegetation indices for LAI and APAR assessment. *Remote Sensing of Environment*, *35*(2–3), 161–173.
- Baret, F., Guyot, G., & Major, D. J. (1989). TSAVI: A vegetation index which minimizes soil brightness effects on LAI and APAR estimation. In: *Proceedings of IGARRS'89. 12th Canadian symposium on remote sensing*, Vancouver, Canada, *3*, (pp. 1355–1358).
- Cai, C. J., Ma, Z. H., Wang, H. G., Zhang, Y. P., & Huang, W. J. (2007). Comparison research of hyperspectral properties between near-ground and high altitude of wheat strip rust. *Acta Phytotopologica Sinica*, *37*, 77–82. (in Chinese).
- Cao, X. R., Luo, Y., Zhou, Y. L., Duan, X. Y., & Cheng, D. F. (2013). Detection of powdery mildew in two winter wheat cultivars using canopy hyperspectral reflectance. *Crop Protection*, *45*, 124–131.
- Carter, G. A., & Miller, R. L. (1994). Early detection of plant stress by digital imaging within narrow stress sensitive wavebands. *Remote Sensing of Environment*, *50*, 295–302.
- Cheng, T., Rivard, B., Sánchez-Azofeifa, G., Feng, J., & Calvo-Polanco, M. (2010). Continuous wavelet analysis for the detection of green attack damage due to mountain pine beetle infestation. *Remote Sensing of Environment*, *114*, 899–910.
- Daughtry, C. S., Walthall, C. L., Kim, M. S., de Colstoun, E. B., & McMurtrey, J. E. (2000). Estimating corn leaf chlorophyll concentration from leaf and canopy reflectance. *Remote Sensing of Environment*, *74*(2), 229–239.
- Franke, J., & Menz, G. (2007). Multi-temporal wheat disease detection by multi-spectral remote sensing. *Precision Agriculture*, *8*, 161–172.

- Gamon, J. A., Penuelas, J., & Field, C. B. (1992). A narrow-waveband spectral index that tracks diurnal changes in photosynthetic efficiency. *Remote Sensing of Environment*, *41*, 35–44.
- Gitelson, A. A., Kaufman, Y. J., & Merzlyak, M. N. (1996). Use of a green channel in remote sensing of global vegetation from EOS-MODIS. *Remote Sensing of Environment*, *58*(3), 289–298.
- Gitelson, A. A., Kaufman, Y. J., Stark, R., & Rundquist, D. (2002). Novel algorithms for remote estimation of vegetation fraction. *Remote Sensing of Environment*, *80*, 76–87.
- Gitelson, A. A., Merzlyak, M. N., & Chivkunova, O. B. (2001). Optical properties and nondestructive estimation of anthocyanin content in plant leaves. *Photochemistry and Photobiology*, *74*(1), 38–45.
- Gong, P., Pu, R. L., & Heald, R. C. (2002). Analysis of in situ hyperspectral data for nutrient estimation of giant sequoia. *International Journal of Remote Sensing*, *23*, 1827–1850.
- Graeff, S., Link, J., & Claupein, W. (2006). Identification of powdery mildew (*Erysiphe graminis* sp. *tritici*) and take-all disease (*Gaeumannomyces graminis* sp. *tritici*) in wheat (*Triticum aestivum* L.) by means of leaf reflectance measurements. *Central European Journal of Biology*, *1*, 275–288.
- Guo, J. B., Huang, C., Wang, H. G., Sun, Z. Y., & Ma, Z. H. (2009). Disease index inversion of wheat stripe rust on different wheat varieties with hyperspectral remote sensing. *Spectroscopy and Spectral Analysis*, *29*, 3353–3357. (in Chinese).
- Haboudane, D., Miller, J. R., Pattey, E., Zarco-Tejada, P. J., & Strachan, I. (2004). Hyperspectral vegetation indices and novel algorithms for predicting green LAI of crop canopies: modeling and validation in the context of precision agriculture. *Remote Sensing of Environment*, *90*, 337–352.
- Herrmann, I., Pimstein, A., Karnieli, A., Cohen, Y., Alchanatis, V., & Bonfil, D. J. (2011). LAI assessment of wheat and potato crops by VEN mu S and Sentinel-2 bands. *Remote Sensing of Environment*, *115*, 2141–2151.
- Huang, W. J., David, W. L., Niu, Z., Zhang, Y. J., Liu, L. Y., & Wang, J. H. (2007). Identification of yellow rust in wheat using in situ spectral reflectance measurements and airborne hyperspectral imaging. *Precision Agriculture*, *8*, 187–197.
- Huete, A. R. (1988). A soil adjusted vegetation index (SAVI). *Remote Sensing of Environment*, *25*, 295–309.
- Jing, X., Huang, W. J., Wang, J. H., Wang, J. D., & Wang, K. R. (2009). Hyperspectral inversion models on verticillium wilt severity of cotton leaf. *Spectroscopy and Spectral Analysis*, *29*, 3348–3352. (in Chinese).
- Kobayashi, T., Kanda, E., Kitada, K., Ishiguro, K., & Torigoe, Y. (2001). Detection of rice panicle blast with multi-spectral radiometer and the potential of using airborne multi-spectral scanner. *Phytopathology*, *91*, 316–323.
- Kokaly, R. F., & Clark, R. N. (1999). Spectroscopic determination of leaf biochemistry using band-depth analysis of absorption features and stepwise multiple linear regression. *Remote Sensing of Environment*, *67*, 267–287.
- Li, F., Mistele, B., Hu, Y. C., Chen, X. P., & Schmidhalter, U. (2014). Reflectance estimation of canopy nitrogen content in winter wheat using optimised hyperspectral spectral indices and partial least squares regression. *European Journal of Agronomy*, *52*, 198–209.
- Liu, L. Y., Huang, W. J., Pu, R. L., & Wang, J. H. (2014). Detection of internal leaf structure deterioration using a new spectral ratio index in the near-infrared shoulder region. *Journal of Integrative Agriculture*, *13*, 760–769.
- Luo, J. H., Huang, W. J., Yuan, L., Zhao, C. J., Du, S. Z., Zhang, J. C., et al. (2013). Evaluation of spectral indices and continuous wavelet analysis to quantify aphid infestation in wheat. *Precision Agriculture*, *14*, 151–161.
- Mahlein, A. K., Rumpf, T., Welke, P., Dehne, H. W., Plümer, L., Steiner, U., et al. (2013). Development of spectral indices for detecting and identifying plant diseases. *Remote Sensing Environment*, *128*, 21–30.
- Maxwell, J. J., Lyerly, J. H., Cowger, C., Marshall, D., Brown-Guedira, G., & Murphy, J. P. (2009). MIAG12: a *Triticum timopheevii*-derived powdery mildew resistance gene in common wheat on chromosome 7AL. *Theoretical and Applied Genetics*, *119*, 1489–1495.
- Merton, R., & Huntington, J. (1999). Early simulation of the ARIES-1 satellite sensor for multi-temporal vegetation research derived from AVIRIS. In *Summaries of the Eight JPL Airborne Earth Science Workshop. JPL Publication, Pasadena, CA* (pp. 299–307)
- Merzlyak, M. N., Gitelson, A. A., Chivkunova, O. B., & Rakitin, V. Y. (1999). Non-destructive optical detection of pigment changes during leaf senescence and fruit ripening. *Plant Physiology*, *106*, 135–141.
- Miller, J. R., Hare, E. W., & Wu, J. (1990). Quantitative characterization of the vegetation red edge reflectance: I. An inverted-Gaussian reflectance model. *International Journal of Remote Sensing*, *11*, 1755–1773.

- Oumar, Z., Mutanga, O., & Ismail, R. (2013). Predicting *Thaumastocoris peregrinus* damage using narrow band normalized indices and hyperspectral indices using field spectra resampled to the Hyperion sensor. *International Journal of Applied Earth Observation Geoinformation*, 21, 113–121.
- Naidu, R. A., Perry, E. M., Pierce, F. J., & Mekuria, T. (2009). The potential of spectral reflectance technique for the detection of Grapevine leafroll-associated virus-3 in two red-berried wine grape cultivars. *Computers and Electronics in Agriculture*, 66(1), 38–45.
- Peñuelas, J., Baret, F., & Filella, I. (1995). Semi-empirical indices to assess carotenoids/chlorophyll a ratio from leaf spectral reflectance. *Photosynthetica*, 31, 221–230.
- Peñuelas, J., Pinol, J., Ogaya, R., & Filella, I. (1997). Estimation of plantwater concentration by the reflectance water index wi (r900/r970). *International Journal of Remote Sensing*, 18, 2869–2875.
- Qi, J., Chehbouni, A., Huete, A. R., Kerr, Y. H., & Sorooshian, S. (1994). Modified soil adjusted vegetation index (MSAVI). *Remote Sensing of Environment*, 48, 119–126.
- Raikes, C., & Burpee, L. (1998). Use of multispectral radiometry for assessment of rhizoctonia blight in creeping bentgrass. *Phytopathology*, 88, 446–449.
- Sankaran, S., Mishra, A., Ehsani, R., & Davis, C. (2010). A review of advanced techniques for detecting plant diseases. *Computers and Electronics in Agriculture*, 72, 1–13.
- Sharma, A. K., Sharma, R. K., & Srinivasa Babu, K. (2004). Effect of planting options and irrigation schedules on development of powdery mildew and yield of wheat in the North Western plains of India. *Crop Protection*, 23, 249–253.
- Sims, D. A., & Gamon, J. A. (2002). Relationships between leaf pigment content and spectral reflectance across a wide range of species, leaf structures and developmental stages. *Remote Sensing of Environment*, 81, 337–354.
- Steddom, K., Heidel, G., Jones, D., & Rush, C. M. (2003). Remote detection of rhizomania in sugar beets. *Phytopathology*, 93(6), 720–726.
- Tian, Y. C., Yao, X., Yang, J., Cao, W. X., Hannaway, D. B., & Zhu, Y. (2011). Assessing newly developed and published vegetation indices for estimating rice leaf nitrogen concentration with ground- and space-based hyperspectral reflectance. *Field Crop Research*, 120, 299–310.
- Turton, B. C. H. (1992). A novel variant of the Savitzky-Golay filter for spectroscopic applications. *Measurement Science and Technology*, 3, 858–863.
- Wang, D. H., Dowell, F. E., Lan, Y. F., Pasikatan, M., & Maghirang, E. (2002). Determining pecky rice kernels using visible and near-infrared spectroscopy. *International Journal of Food Properties*, 5, 629–639.
- West, J. S., Bravo, C., Oberti, R., Lemaire, D., Moushou, D., & McCartney, H. A. (2003). The potential of optical canopy measurement for targeted control of field crop diseases. *Annual review of Phytopathology*, 41, 593–614.
- Yang, C. M., Cheng, C. H., & Chen, R. K. (2007). Changes in spectral characteristics of rice canopy infest with brown planthopper and leafhopper. *Crop Science*, 47(1), 329–335.
- Yang, Z., Rao, M. N., Elliott, N. C., Kindler, S. D., & Popham, T. W. (2009). Differentiating stress induced by greenbugs and Russian wheat aphids in wheat using remote sensing. *Computers and Electronics in Agriculture*, 67, 64–70.
- Yoshio, I., Eiji, S., Zhu, Y., & Wataru, T. (2012). Diagnostic mapping of canopy nitrogen content in rice based on hyperspectral measurements. *Remote Sensing of Environment*, 126, 210–221.
- Zhang, J., Pu, R., Huang, W., Lin, Y., Luo, J., & Wang, J. (2012a). Using in situ hyperspectral data for detecting and discriminating yellow rust disease from nutrient stresses. *Field Crops Research*, 134(3), 165–174.
- Zhang, J. C., Pu, R. L., Wang, J. H., Huang, W. J., Yuan, L., & Luo, J. H. (2012b). Detecting powdery mildew of winter wheat using leaf level hyperspectral measurements. *Computers and Electronics in Agriculture*, 85, 13–23.
- Zhang, J. C., Pu, R. L., Yuan, L., Wang, J. H., Huang, W. J., & Yang, G. J. (2014). Monitoring powdery mildew of winter wheat by using moderate resolution multi-temporal satellite imagery. *PLoS ONE*, 9, 93–107.
- Zhang, M. H., Qin, Z. H., Liu, X., & Ustin, S. L. (2003). Detection of stress in tomatoes induced by late blight disease in California, USA, using hyperspectral remote sensing. *International Journal of Applied Earth Observation and Geoinformation*, 4, 295–310.